JMEPEG (2012) 21:1030–1039
DOI: 10.1007/s11665-011-9995-z

1059-9495/$19.00

Phase Transformations and Microstructural Observations During Subcritical Heat Treatments of a High-Chromium Cast Iron

A.E. Karantzalis, A. Lekatou, A. Kapoglou, H. Mavros, and V. Dracopoulos

(Submitted June 9, 2010; in revised form February 16, 2011)

In this study, Cr white iron of 18.23 wt.% was subjected to a series of subcritical heat treatments. At both temperatures of 350 and 450 °C, no precipitation of secondary carbides was observed, and the overall microstructure resembles to that of the as-cast condition. At 550 °C, hardness values increased slightly compared to the as-cast values. No evidence of secondary carbide formation was observed. At 650 and 750 °C, extensive-to-complete transformation to pearlite-ferrite structures has occurred. Some evidence of secondary carbide precipitation especially for prolonged treatment periods was not adequate to obstruct the hardness decrease due to the dominating effect of pearlitic-ferritic formation. At 850 °C, secondary carbide precipitation and martensite formation lead to high hardness values.

Keywords cast iron, high chromium, secondary carbides, subcritical treatment

1. Introduction

High-chromium white cast irons are well-established materials of choice for applications wherein exceptional abrasion wear and corrosion resistance, absorption ability of high vibration, and good heavy load transfer application behavior are demanded. These characteristics are mainly associated with the various phases present in their microstructure. Tabrett and Sare (Ref 1), in their extensive review, address all the key issues that can control and modify the microstructure of these materials. Especially, as far as the relation between microstructure and resistance to abrasion wear is concerned, the reader should refer to the studies of Tabrett and Sare (Ref 1) and Dogan and coworkers (Ref 2-4).

The typical as-cast microstructure of these alloys consists of primary austenitic dendrites and an austenite/M_7C_3 (usually referred as primary or eutectic) eutectic mixture. Detailed examinations of the microstructure of high-chromium white cast irons have been described by Maratray and Poulalion (Ref 5).

High-chromium white cast irons can be subjected to two main types of heat treatment: a) Destabilization (or critical) heat treatments (heating at 800-1100 °C for 1-6 h; Ref 1-5), aiming at destabilizing the highly alloyed austenitic matrix to transform into martensite during cooling. They also intend to cause secondary carbide precipitation. b) Subcritical heat treatments (200-600 °C for 2-6 h; Ref 3-5), usually after destabilization treatments with the purpose of further precipitation of secondary carbides and elimination of any retained austenitic phase after the destabilization treatment.

Despite extensive experimental effort having been conducted to clarify the involved mechanisms of the microstructural modifications during the sequence of destabilization-subcritical heat treatments, only limited amount of study has been focused on the direct application of subcritical heat treatments of high-chromium white cast irons. It has been reported (Ref 1-6) that during such treatments, the highly alloyed metastable austenitic matrix can be decomposed into various combinations of ferritic and secondary carbide phases with the primary M_7C_3 phase being practically unaffected.

Wang (Ref 7) studied the behavior of a 16Cr-1Mo-1Cu white cast iron during subcritical treatment at 853 K (580 °C) for different time intervals of processing. A sharp hardness increase was observed between 2 and 10 h, followed by a smooth drop for the next 6 h. Above 16 h of processing, a slight increase was observed. These hardness fluctuations were associated with the different microstructural features. Wang et al. (Ref 8) studied the effects of precipitation and transformation of secondary carbides on the hardness of a 15Cr-1Mo-1.5V white cast iron under a subcritical treatment. Heating at 833 K (560 °C) led to two hardness peaks, after 10 h and 14 h, respectively. The first peak was attributed to martensitic transformation and $M_{23}C_6$ precipitation. The second peak was associated with the presence of MoC, $(Cr,V)_2C$, and $M_{23}C_6$ carbides.

This study is part of a wider investigation of the heat treatments of high-chromium white irons (Ref 9-13), aiming at clarifying their effect on the microstructure and, consequently, the properties of these materials. The final target is to develop a sound database of the possible treatments, fully and accurately characterized, so as to select the optimum (microstructure, properties, and cost) treatment for a specific application.

A.E. Karantzalis, A. Lekatou, A. Kapoglou, and **H. Mavros**, Laboratory of Applied Metallurgy, Department of Materials Science and Engineering, University of Ioannina, University Campus, 45110 Ioannina, Hellas, Greece; and **V. Dracopoulos**, Institute of Chemical Engineering and High Temperature Chemical Processes, Foundation for Research and Technology Hellas (ICEHT/FORTH), Stadiou Street, 26500 Patra, Hellas, Greece. Contact e-mails: alekatou@cc.uoi.gr and alexkarantzalis@gmail.com.

Previous study (Ref 9) investigated the effects of the sequence reversal of destabilization-subcritical heat treatments (D-S and S-D) on the microstructure of a white cast iron. D-S leads to lower hardness values than S-D because of pearlite-secondary carbides-modified primary carbides in comparison with martensite-secondary carbides obtained after the reversal treatment. This study was complemented by an investigation on the effect of alloying additions (Mo, Cr, Si, and C) on the microstructure of treated irons (Ref 10). Application of solely destabilization treatments in the range of 800-1100 °C (Ref 11) determined the optimum destabilization temperature for the highest hardness, associated with the stoichiometry and morphology of the secondary carbides formed.

Karantzalis et al. (Ref 9) during their primary investigation of a subcritical heat treatment (600 °C and 13 h) observed interesting combinations of strong and ductile features. Therefore, the scope of the present study is to further investigate the effect of just subcritical treatments on the microstructure and hardness of a selected high-Cr white cast iron in an effort to minimize the cost of a destabilization-subcritical treatment combination.

2. Experimental Procedure

The examined high-chromium white cast iron consists of 2.35 wt.% C, 18.23 wt.% Cr, 0.46 wt.% Mo, 0.61 wt.% Si, 0.62 wt.% Mn, 0.0028 wt.% P, and Fe the balance. The material was prepared by melting the appropriate raw material in an induction furnace. Casting was then performed in bentonite sand molds, at the temperature range of 1440-1460 °C. The specimens were cut off and subjected to subcritical heat treatments at 350, 450, 550, 650, 750, and 850 °C for 30, 60, 120, 180, 240, 360, 480, 600, 720, 840, 960, 1080, 1200, 1800, 1920, and 2040 min followed by cooling in air. Although the temperature of 850 °C is considered as a destabilization temperature, it was adopted for comparison to the subcritical treatments reasons.

Specimens were mounted, ground, and polished according to standard metallographic procedure and chemically etched by a solution containing 94 mL CH_3CH_2OH, 5 mL HCl and 1 g $C_6H_3N_3O_7$ acid. The hardness test was performed by a portable hardness tester (Equotip brand, five measurements per cm^2 of specimen area). The microstructure was examined using an optical microscope (Leica 4000 DM type) and SEM (Zeiss Supra 35VP SEM equipped with a Roentec Quantax (Bruker AXs) EDS system, and JEOL 5600 SEM system equipped with an Oxford Instruments EDS system). Microhardness measurements were conducted using a Shimadzu HMV tester.

3. Results and Discussion

Figure 1 shows the hardness values for the different heat treatments. In the following paragraphs, an effort to correlate hardness and microstructure is attempted.

3.1 As-Cast Alloy

The microstructure of the as-cast alloy is presented in Fig. 2(a). Large metastable austenitic dendrites, surrounded by a eutectic mixture of austenite/M_7C_3 are observed. This morphology agrees with previous experimental findings (Ref 1-6, 9-13). In the eutectic mixture, a black layer enveloping the eutectic carbide at the austenite/carbide interface is discerned. The presence of this black layer is linked (Ref 1-6, 9-13) with the formation of a thin martensitic layer close to the vicinity of the primary carbides. The mechanism of such martensite formation has been described as follows (Ref 1): the formation of the primary carbide phases causes the local depletion of the austenitic phase from alloying additions and carbon. Such depletion raises the M_s temperature of the affected austenitic area and, hence, the latter is transformed to martensite upon cooling. As will be presented later, the characteristic γ/M_7C_3 eutectic morphology may be confusing and possibly misleading in cases where phase transformation (especially γ to ferrite/pearlite) is concerned. Microhardness measurements of the eutectic area gave values of 565 ± 10 $HV_{0.5}$. This value will be used later on for comparison reasons. Figure 2(b) shows a characteristic microhardness trace on the examined (eutectic) area.

3.2 Heat Treatments at 350 and 450 °C

Figure 3(a) and (b) shows the microstructure of specimens treated at 350 °C for 120 min and 1800 min, respectively. Figure 4(a) and (b) presents the microstructure of the specimens treated for 120 min and 1800 min, respectively, at 450 °C. The microstructure has more or less remained the same as in the cast condition: large austenitic dendrites

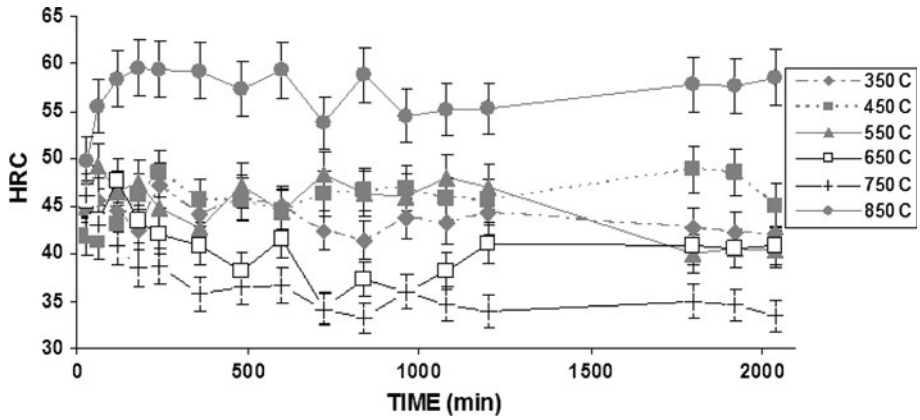

Fig. 1 Hardness values vs. time for the different heat treatments of the alloy

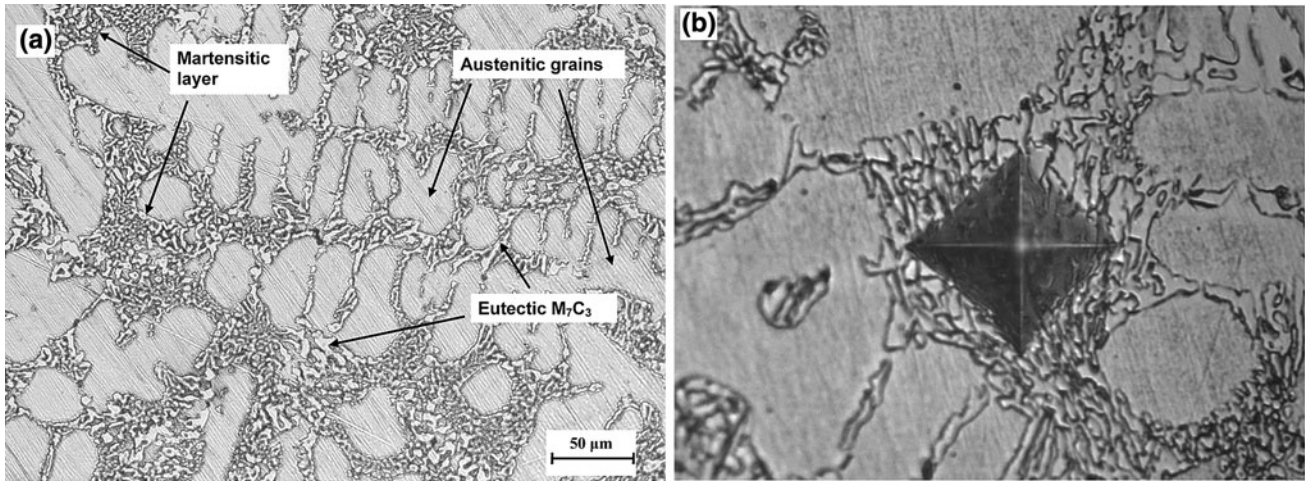

Fig. 2 (a) Microstructure of the as-cast alloy: austenitic grains along with eutectic M_7C_3 carbide are observed. A dark thin martensitic layer surrounding the eutectic carbide phase can also be discerned. (b) Typical microhardness trace at the area of eutectic mixture

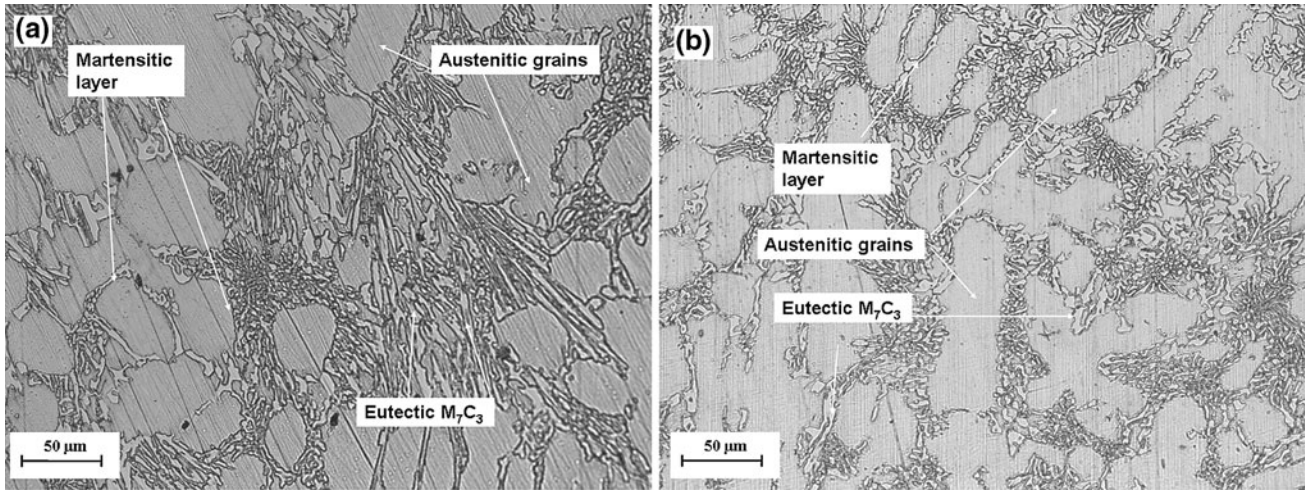

Fig. 3 Microstructure of the alloy treated at 350 °C: (a) after 120 min and (b) after 1800 min. The morphological features are similar to that of the as-cast material comprising austenite grains, eutectic carbides, and a thin martensitic layer

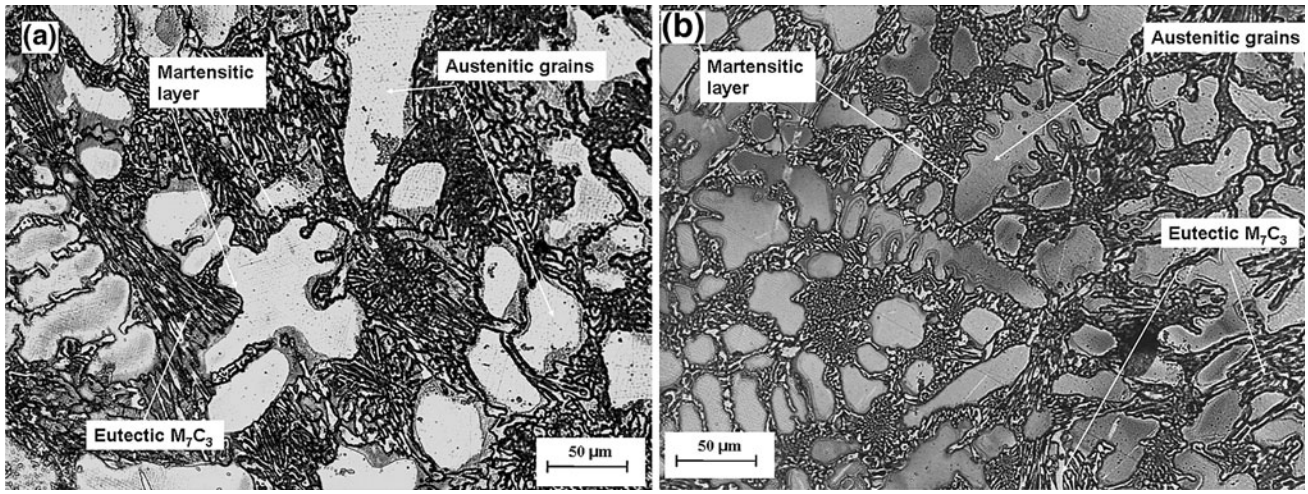

Fig. 4 Microstructure of the alloy treated at 450 °C: (a) after 120 min and (b) after 1800 min. No significant change on the microstructural features is observed

surrounded by an austenite/primary M_7C_3 eutectic mixture. Further examination with SEM verified these findings. Figure 5(a) and (b) shows the microstructure of the alloy treated at 450 °C for 360 and 1080 min, respectively. Neither secondary carbide precipitation nor austenitic dendrite transformation is observed.

As far as the hardness is concerned, Fig. 1 shows that there are, in general, no significant differences with the values of the as-cast condition. Some degree of value fluctuation, especially for short- and medium-processing times can nevertheless be observed. This is possibly attributed to various competing phenomena such as

(a) Internal stress relief that can cause hardness reduction especially at the early stages of treatment.
(b) Tempering of martensite formed during the casting of the alloy. As described in the morphology of the casting alloy, a thin layer of martensitic phase envelops the eutectic carbide areas. This martensite is practically subjected, during heat treatment, to tempering conditions. Such a tempering process can lead to various microstructural modifications, such as metastable ε-carbide formation, cementite formation, tempered martensite, etc. The nature and the degree of the formed phases is a function of time, temperature, and composition parameters (Ref 1). Although martensite tempering leads to a decrease in hardness, the formation of ε-carbide at the first stages of tempering may cause an increase in hardness. Furthermore, retained austenite may be released by tempering, and it subsequently transforms to bainite or martensite (the latter upon cooling). These transformations enhance the hardness. The higher diffusion rates at 450 °C as compared to 350 °C intensified martempering and, subsequently, the bainite and/or quench-induced martensite formation. Thus, treatment at 450 °C eventually (>500 min) results in higher hardness than the 350 °C treatment. Hence, it can be postulated that the diffusion processes at $t > 500$ min are governed most likely by the release of the retained austenite rather than martempering. It should be noticed that the low occurrence of martensite in the as-cast alloy may account for the low differences of the hardness values, as well as the slightly higher hardness of the 450 °C-treated alloy in relation to the 350 °C-treated alloy.

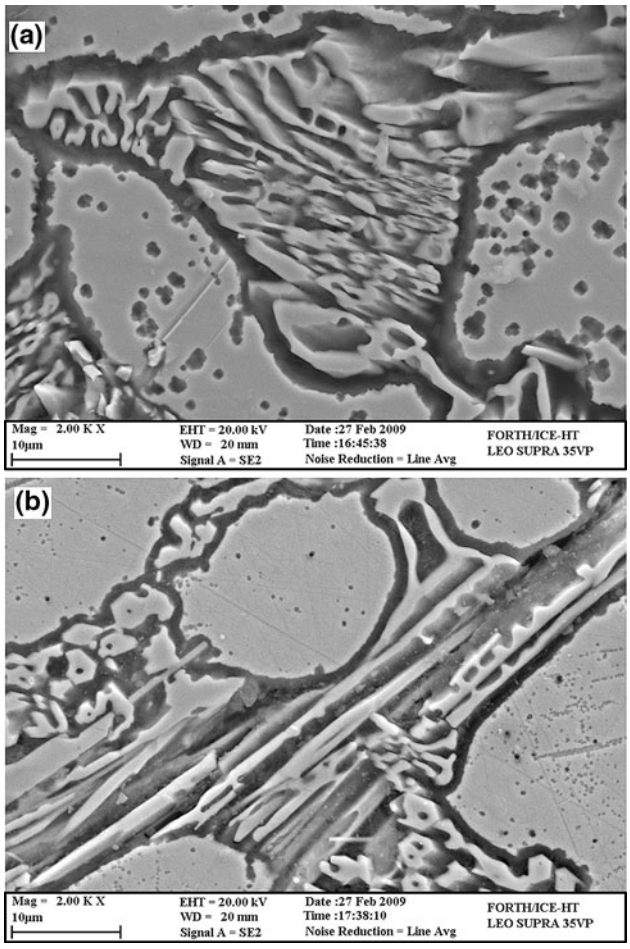

Fig. 5 Microstructure of the alloy treated at 450 °C under SEM: (a) after 360 min and (b) after 1080 min. No significant evidence of secondary carbide formation is observed

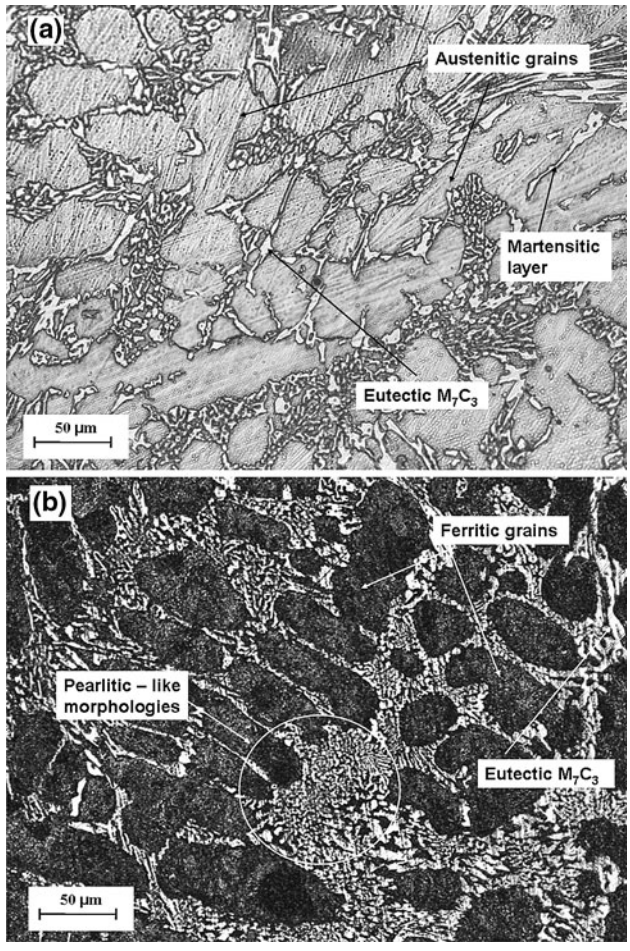

Fig. 6 Microstructure of the alloy treated at 550 °C. (a) After 120 min: no considerable change in the morphological features can be observed. Microstructure consists of austenitic dendrites, eutectic M_7C_3, and a thin martensitic layer. (b) After 1800 min: microstructure is significantly changed compared to that of the as-cast structure and consists of ferritic grains, pearlitic-like morphologies and eutectic carbide phases

It becomes clear, thus, that the exact mechanisms to explain the hardness fluctuations can be rather complicated, for ascertaining which examination at higher depth is required, which has not been adopted in the present effort.

3.3 Heat Treatment at 550 °C

Figure 6(a) and (b) presents the microstructure of specimens treated at 550 °C for 120 and 1800 min, respectively. For the short-processing times (Fig. 6a), no significant alterations are observed in the microstructure. The latter consists of austenitic grains and eutectic mixture of M_7C_3/austenite. After 1800 min of treatment (Fig. 6b), however, the microstructure has significantly changed. An extensive transformation of austenite to ferrite has occured. Pearlite-like structures have also a considerable presence. Closer examination under SEM (Fig. 7a, b) of specimens treated at 550 °C for 360 and 1080 min, respectively, has failed to reveal any trace of secondary carbide precipitation. Same observations can be made for higher magnifications (Fig. 7c, d).

Hardness values (Fig. 1) show no considerable changes to that of the as-cast state at least for short, medium, and medium-to-prolonged times of treatment. The slight decrease observed for prolonged treatment periods can be associated with ferritic-pearlitic-like structure formations along with phase-coarsening phenomena. It should be noticed, however, that such morphologies may not be of pearlitic nature but eutectic γ/M_7C_3 mixture persisting from the as-cast material of a different orientation. Indeed, microhardness measurements revealed values of 555 ± 15 $HV_{0.5}$ which do not differ significantly form the eutectic values of 565 ± 10 $HV_{0.5}$ presented earlier. Thus, the slight decrease of overall hardness may be attributed to the coarsening phenomena. Wang (Ref 7) observed the formation of pearlitic structures for extensive treatment (>960 min) at 560 °C. However, Wang (Ref 7) also observed the simultaneous precipitation of secondary carbides at the same conditions through the use of TEM examination. In the present experimental findings, no such precipitation was observed, yet no TEM analysis was facilitated. Wang (Ref 7) also observed the formation of martensite for intermediate treatment times (300-900 min) which has not been adopted in this study, since such formation should have led to a drastic hardness increase. It is possible to attribute such difference in behavior to the different Cr and C contents: The high Cr and C contents of the examined alloy can result in a higher M_s temperature (Ref 14, 15). Moreover, the enhanced stability of austenite may retard the γ to pearlite transformation initiation.

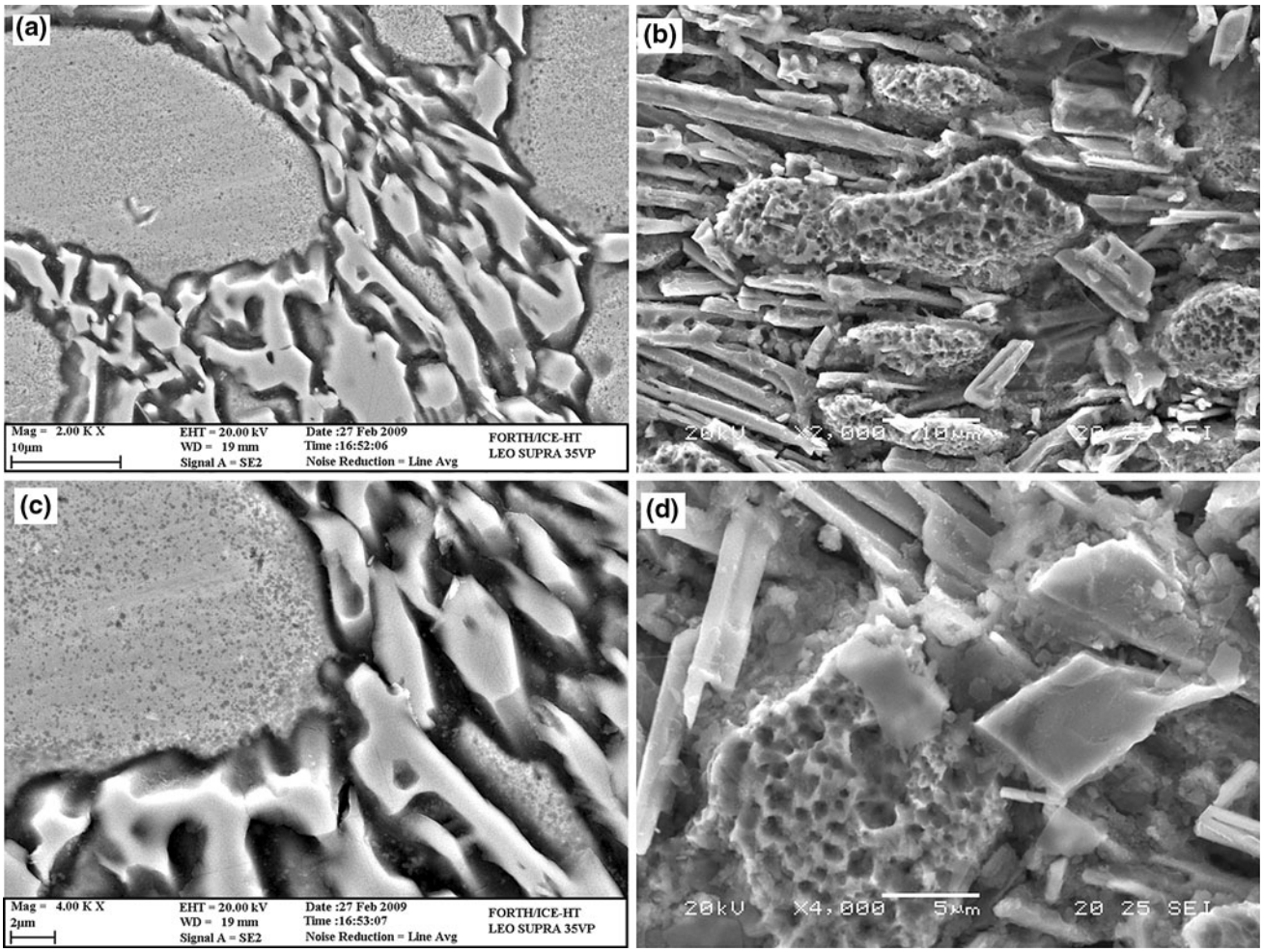

Fig. 7 Microstructure of the alloy treated at 550 °C under SEM examination: (a, c) after 360 min and (b, d) after 1080 min. No significant evidence of secondary carbide precipitation can be observed

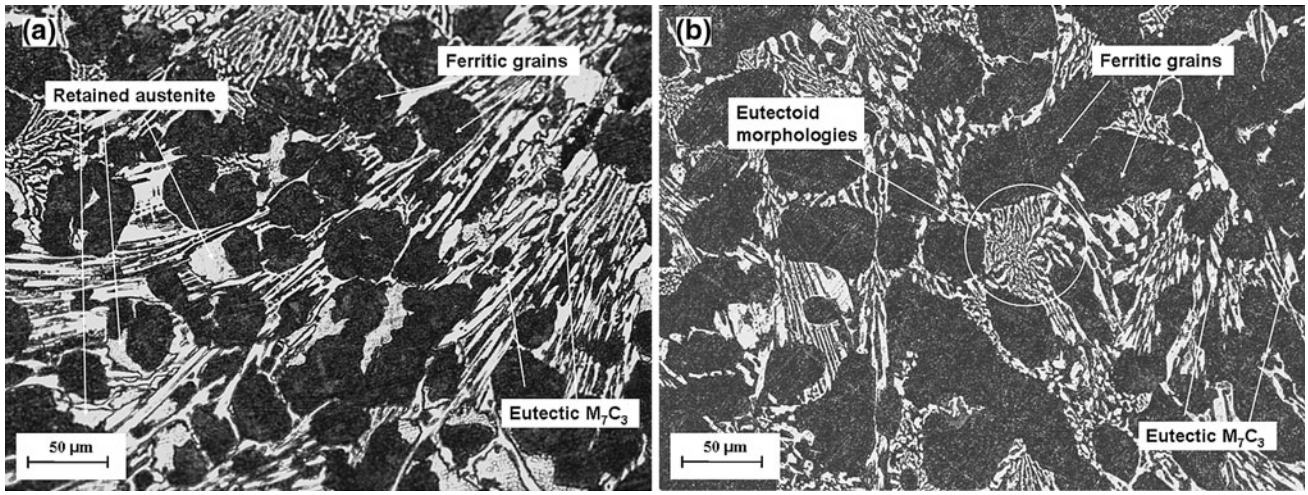

Fig. 8 Microstructure of the alloy treated at 650 °C. (a) After 120 min: microstructrure consists of ferritic grains, retained austenite, pearlitic structures, and eutectic carbide phases. (b) After 1800 min: microstructure consists of ferritic grains, eutectoid morphologies (possibly pearlitic) and eutectic carbides

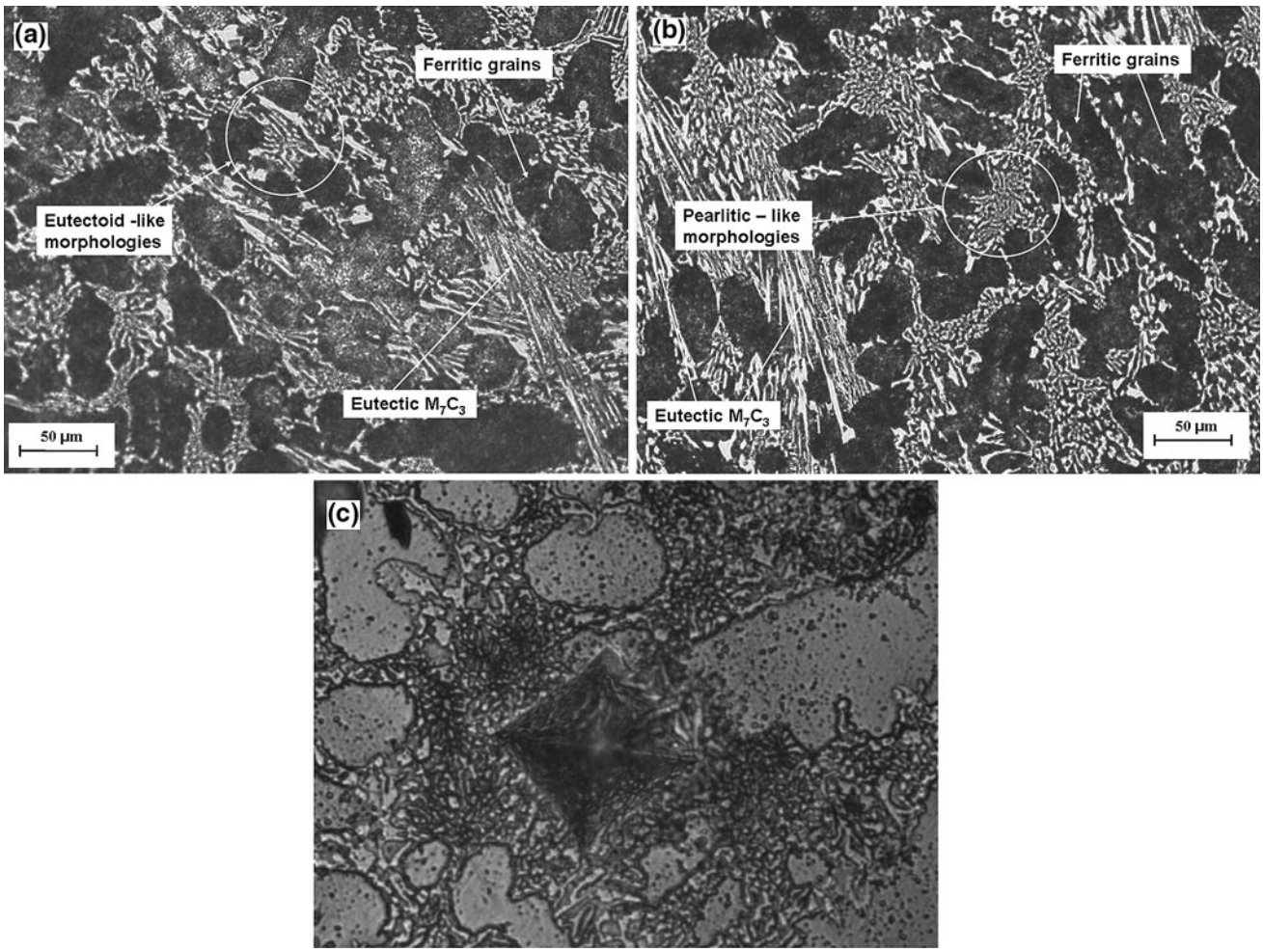

Fig. 9 Microstructure of the alloy treated at 750 °C: (a) after 120 min and (b) after 1800 min. In both cases, the microstructure consists of ferritic grains, eutectoid like (possibly pearlitic) morphologies and eutectic carbide phases, and (c) microhardness traces at the area of the possible pearlitic morphology

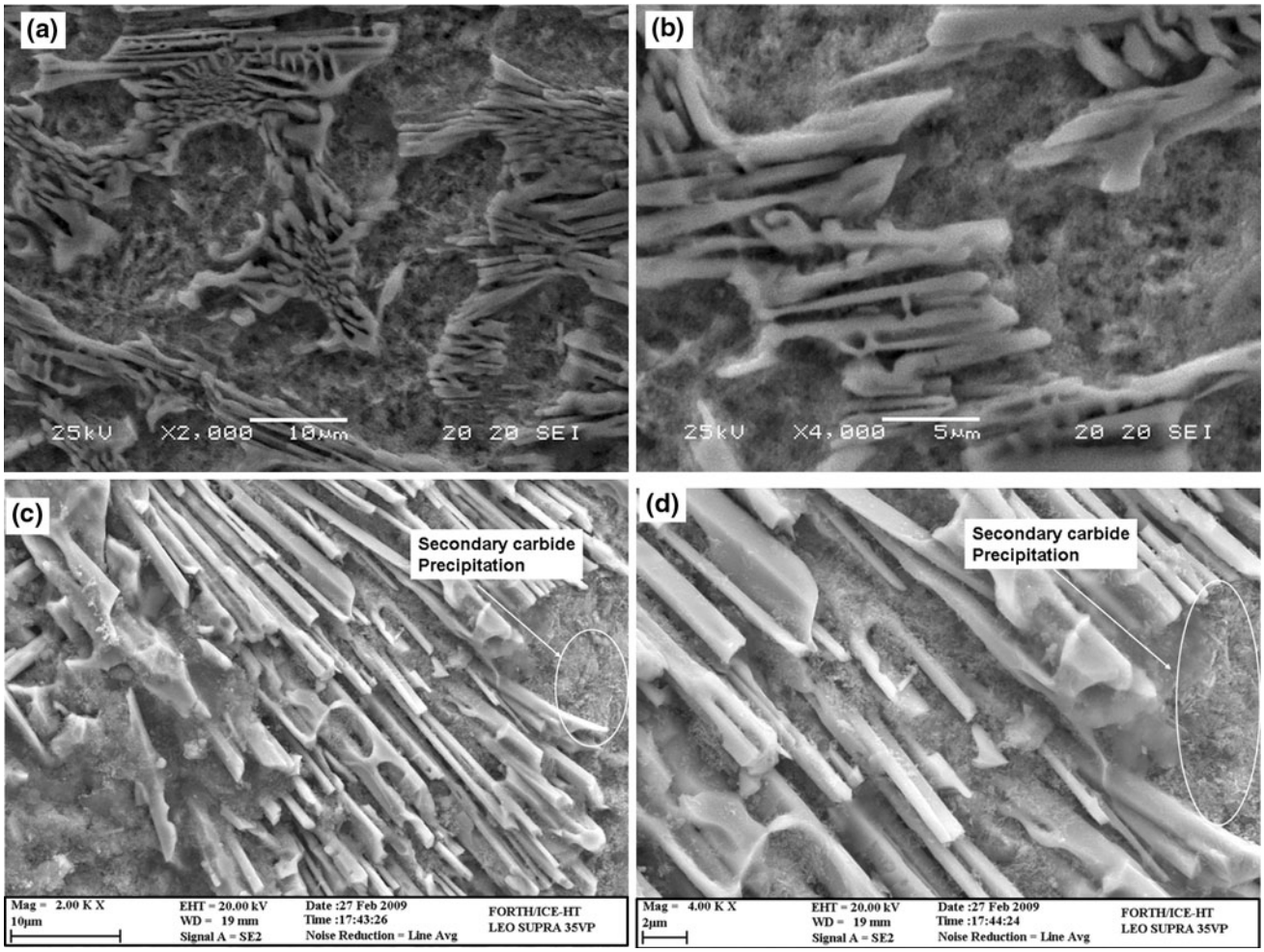

Fig. 10 Microstructure of the alloy treated at 650 °C under SEM. (a, b) After 360 min: no significant evidence of secondary carbide precipitation can be observed. (c, d) After 1080 min: areas of possible secondary carbide precipitation can be observed

3.4 Heat Treatment at 650-750 °C

Previous experimental efforts (Ref 1-3, 7, 8) have shown that treatment at temperatures above 600 °C can cause austenite transformation to various combinations of α-ferrite, pearlite-like and/or α + other carbides. Such transformations result in hardness decrease. Gundlach and Parks (Ref 16) report hardness values of 70-200 HV, 250-320 HV and 300-600 HV for ferrite, perlite and high Cr austenite respectively. Asensio et al. (Ref 17) report hardness values of 240-450 and 350-400 HV for high carbon pearlite and alloyed austenite respectively. Taking into account these values, it is thoughtful to postulate that a combination of α + pearlite should lead to hardness values lower than that of a highly alloyed austenite. The hardness values, presented in Fig. 1, appear to validate the above statement, as both subcritical treatments (650 and 750 °C) have resulted in lower hardness as compared with the treatments at 350, 450, and 550 °C.

Figure 8(a) and (b) shows the microstructure of specimens treated at 650 °C, after 2 and 30 h, respectively, and Fig. 9(a) and (b) presents the microstructure of specimens after treatment at 750 °C, also for 2 and 30 h, respectively. It is observed that for short-processing times (Fig. 8a, 9a), the austenitic phase has partially been transformed to ferritic and pearlitic-like structures, whereas, for prolonged treatment times, the transformation of austenite is complete (Fig. 8b, 9b). However, as already mentioned above, the eutectoid pearlitic morphology can be easily confusing so as to mislead us to be that of the eutectic γ/M_7C_3 as cast mixture. Microhardness measurements of the pearlitic-like morphologies for 650 °C/30 h, 750 °C/2 h, and 750 °C/30 h specimens revealed values of 439 ± 10, 437 ± 15, and 368 ± 12 $HV_{0.5,}$ respectively. Such values do confirm the presence of the softer-to-the eutectic γ/M_7C_3 pearlitic phase. Figure 9(c) shows an example of the microhardness trace on the area of pearlitic morphology. Closer examination of the microstructures under SEM reveals, however, some interesting features. Figure 10(a) and (b) shows the microstructure of a specimen treated at 650 °C for 360 min. Figure 10(c) and (d) presents the microstructure of specimen treated at 650 °C for 1080 min. Although for the shorter treatment periods, any significant evidence of secondary carbide precipitation cannot be observed, for the prolonged times, there are some formations within the ferritic regions that resemble to the presence and the structure of secondary carbides. However, it was proved

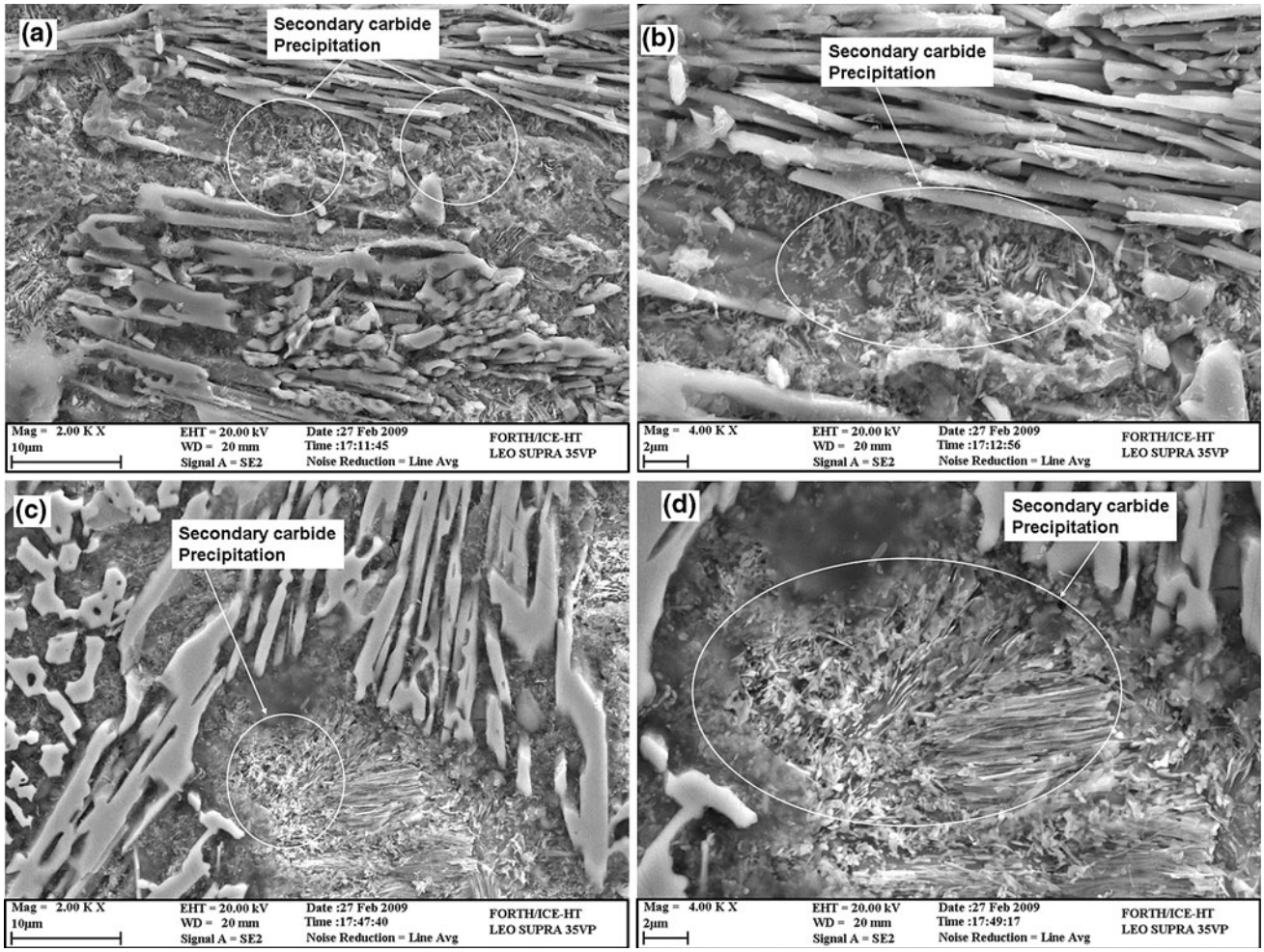

Fig. 11 Microstructure of the alloy treated at 750 °C under SEM examination: (a, b) after 360 min and (c, d) after 1080 min. In all the cases, areas of secondary carbide precipitation can be observed

very difficult to identify the stoichiometry of such phases through EDX analysis because of their very fine size. Nevertheless, at such prolonged times of treatment, it is unlikely for $M_{23}C_6$ to be retained; the M_7C_3 formation is more thermodynamically favourable (Ref 7, 8). Similar observations can be made for the specimens treated at 750 °C (Fig. 11a-d). The major difference is that the presence of the carbide phases are even observed at medium-processing times (360 min). Similar to the fore-mentioned considerations, the morphologies of the carbide phases most likely correspond to the M_7C_3 type.

However, Fig. 1 shows a continuous drop in the hardness values up to ~960 min, which is in consistency with the progress of $\gamma \rightarrow \alpha$ + pearlite transformation as well as grain growth. The hardness increase after 960 min may be justified by the formation and progress of the secondary carbide phase. However, the generally lower hardness of the alloy treated at 750 °C as compared with the alloy heated at 650 °C may be attributed to both the extent of ferrite-perlite formation and the degree of grain growth/coarsening phenomena. Such coarsening phenomena may also account for the primary M_7C_3 carbide phases especially in terms of spherodization process. Primary eutectic carbide spherodization may also contribute to the hardness decrease.

3.5 Heat Treatment at 850 °C

As aforementioned, heat treatment of high-chromium white irons at 850 °C, is more likely a destabilization treatment rather than a subcritical one. However, it was included in the present investigation for the purpose of comparison with the rest of treatments reasons.

Figure 12(a) and (b) presents the microstructure of alloys treated at 850 °C for 120 and 1800 min, respectively. In both cases, severe transformation of the austenitic phase can be observed. Closer examination under SEM (Fig. 13a, b) shows the formation of secondary carbide phases. The morphology, shape, and arrangement of the particles under such conditions have also been reported in other efforts (Ref 1-6, 9-13, 18-20) and indicate most likely a $M_{23}C_6$ stoichiometry. Both the presence of martensite along with the precipitation of secondary carbides are responsible for the high hardness values obtained, considerably higher than the values for the rest of the subcritical heat treatments. The precipitation of secondary carbides causes the depletion of the primary austenitic phase from alloying elements resulting in an increase of the M_s temperature, so that the unstable austenite is transformed into martensite upon cooling. These observations are in agreement with other experimental investigations (Ref 1-6, 9-13, 18-20).

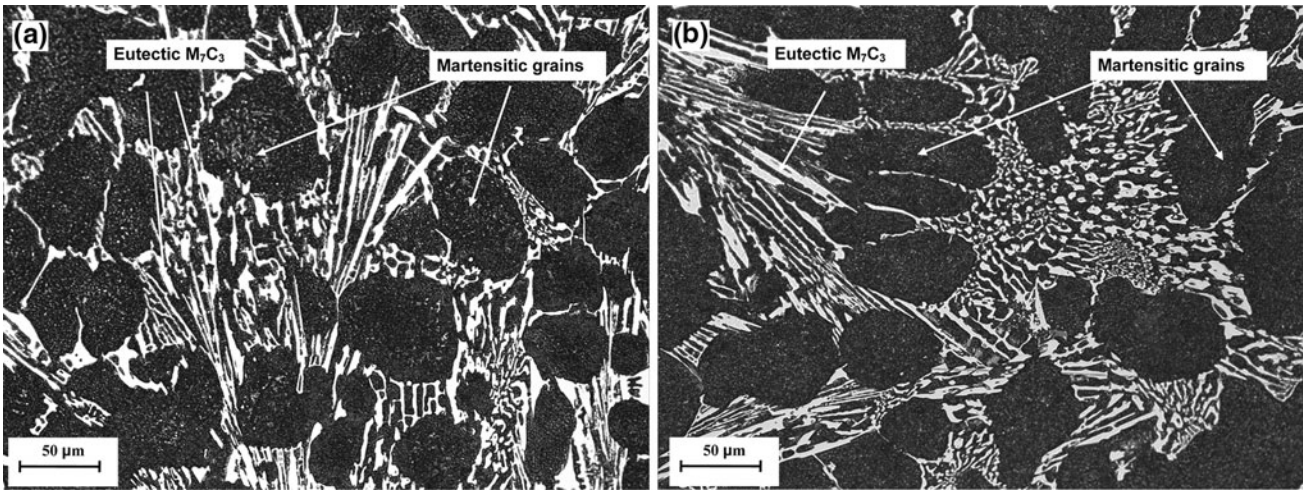

Fig. 12 Microstructure of the alloy treated at 850 °C: (a) after 120 min and (b) after 1800 min. In both cases, martensitic grains, pearlitic-like morphologies and eutectic carbides are observed

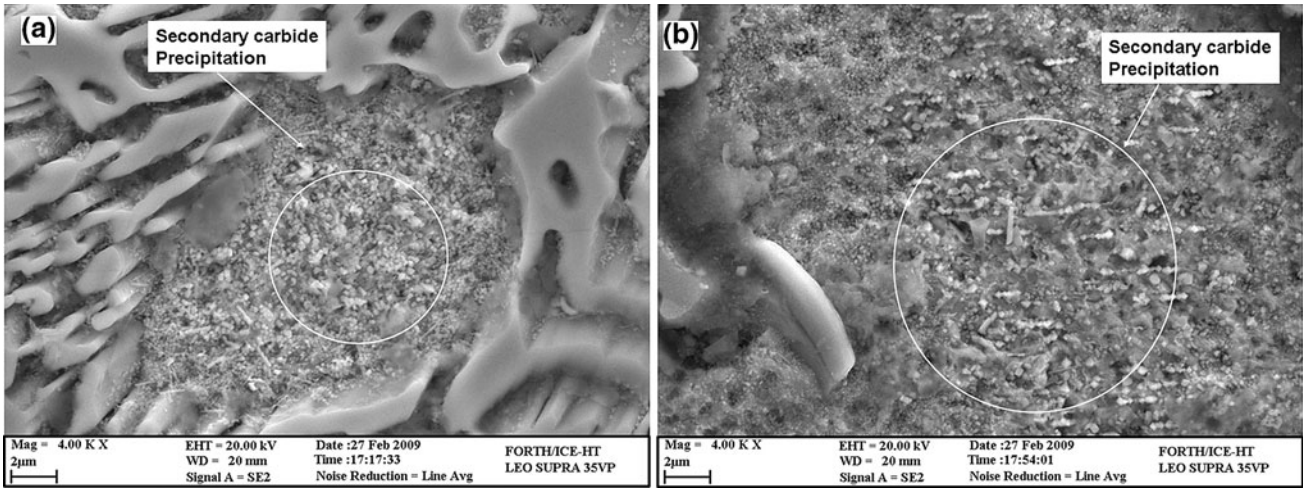

Fig. 13 Microstructure of the alloy treated at 850 °C under SEM examination: (a) after 360 min and (b) after 1080 min. In both cases, precipitation of secondary carbide particles is observed

4. Conclusions

(1) The as-cast alloy consists of large metastable austenitic dendrites, and a eutectic mixture of austenite and primary M_7C_3. The material's hardness is found to be 44 ± 3 HRC.

(2) Treatments at 350 and 450 °C have not caused any change in the microstructure. No precipitation of secondary carbides has been observed. Hardness has not been altered compared to that of the as-cast state. Some fluctuations at the early stages have been attributed to residual stress relief and tempering phenomena.

(3) Microstructural alterations, observed by optical microscopy for treatment at 550 °C for prolonged times, were not proved to be associated with austenite to pearlite-like/ferrite transformation as revealed by microhardness measurements. The slight increase in hardness compared with lower-temperature treatments may be associated with the precipitation of secondary carbide particles.

(4) Treatment at 650 °C has caused an extensive-to-full transformation of austenite to pearlitic/ferritic morphologies. Such microscopy observations were also supported by microhardness measurements. Prolonged treatment has caused precipitation of secondary carbide particles that cannot, however, counterbalance the softening effect of austenite transformation. Similar microstructure of the material is observed at 750 °C. The slightly lower hardness values are attributed to phase coarsening, grain growth, and tempering process.

(5) Heat treatment at 850 °C has led to both martensite formation, and secondary carbide precipitation that drastically increased the hardness levels.

References

1. C.P. Tabrett and I.R. Sare, Effect of High Temperature and Sub-Ambient Treatments on the Matrix Structure and Abrasion Resistance of a High Chromium White Iron, *Scripta Mater.*, 1998, **38**, p 1747–1753
2. O.N. Dogan, J.A. Hawk, and G. Laird, II, Solidification Structure and Abrasion Resistance of High Chromium White Irons, *Met. Mater. Trans.*, 1997, **28**(6), p 1315–1328
3. O.N. Dogan and J.A. Hawk, Effect of Carbide Orientation on Abrasion of High Cr White Cast Iron, *Wear*, 1995, **189**, p 136–142
4. O.N. Dogan, G. Laird, II, and J.A. Hawk, Abrasion Resistance of the Columnar Zone in High Cr White Cast Irons, *Wear*, 1995, **181–183**, p 342–349
5. F. Maratray and A. Poulalion, Austenite Retention in High Chromium White Irons, *Trans. AFS*, 1982, **90**, p 795–804
6. H.X. Chen, Z.C. Chang, J.C. Lu, and H.T. Lin, Effect of Niobium on Wear Resistance of 15% Cr White Cast Iron, *Wear*, 1993, **166**, p 197–201
7. J. Wang, Effects of Secondary Carbides Precipitation and Transformation Abrasion Resistance of the 16Cr-1Mo-1Cu White Iron, *J. Mater. Eng. Perform.*, 2006, **15**, p 316–319
8. J. Wang, R.L. Luo, and Z.P. San, Influence of Secondary Carbides Precipitation and Transformation of Hardening of a 15Cr-1Mo-1.5V White Iron, *Mater. Charact.*, 2005, **55**, p 234–250
9. A.E. Karantzalis, A. Lekatou, and H. Mavros, Microstructural Modifications of As-Cast High Chromium White Iron by Heat Treatment, *J. Mater. Eng. Perform.*, 2009, **18**(2), p 174–181
10. E. Karantzalis, A. Lekatou, and H. Mavros, Microstructure and Properties of High Chromium Cast Irons: Effect of Heat Treatments and Alloying Additions, *Int. J. Cast Met. Res.*, 2009, **22**(6), p 448–456
11. A.E. Karantzalis, A. Lekatou, and L. Diavati, Effect of Destabilization Heat Treatments on the Microstructure of High Chromium Cast Iron: A Microscopy Examination Approach, *J. Mater. Eng. Perform.*, 2009, **18**(8), p 1078–1085
12. J. Wang, C. Li, H. Liu, H. Yang, B. Shen, S. Gao, and S. Huang, The Precipitation and Transformation of Secondary Carbides in a High Chromium Cast Iron, *Mater. Charact.*, 2006, **56**, p 73–78
13. J.T.H. Pearce, Examination of MC_3 Carbides in High Chromium Cast Irons Using Thin Foil Transmission Electron Microscopy, *J. Mater. Sci. Lett.*, 1983, **2**, p 428–432
14. Z. Sun, R. Zuo, C. Li, B. Shen, J. Yan, and S. Huang, TEM Study on Precipitation and Transformation of Secondary Carbides in 16Cr-1Mo-1Cu White Iron Subjected to Subcritical Treatment, *Mater. Charact.*, 2004, **53**(5), p 403–409
15. J.-Y. Park and Y.-S. Park, The Effects of Heat-Treatment Parameters on Corrosion Resistance and Phase Transformations of 14Cr-3Mo Martensitic Stainless Steel, *Mater. Sci. Eng. A*, 2007, **449–451**, p 1131–1134
16. R.B. Gundlach and J.L. Parks, Influence of Abrasive Hardness on the Wear Resistance of High Chromium Irons, *Wear*, 1978, **46**, p 97–108
17. J. Asensio, J.A. Pero-Sanz, and J.I. Verdela, Microstructure Selection Criteria for Cast Irons with More Than 10 wt.% Chromium for Wear Applications, *Mater. Charact.*, 2003, **49**, p 83–93
18. G.L.F. Powell and G. Laird, II, Structure, Nucleation, Growth and Morphology of Secondary Carbides in High Chromium and Cr-Ni White Cast Iron, *J. Mater. Sci.*, 1992, **27**, p 19–35
19. A. Wiengmoon, T. Chairuangsri, and J.T.H. Pearce, An Unusual Structure of an As-Cast 30% Cr Alloy White Iron, *ISIJ Int.*, 2005, **45**, p 1658–1665
20. G.L.F. Powell and J.V. Bee, Secondary Carbide Precipitation in an 18 wt.%Cr-1 wt.%Mo White Iron, *J. Mater. Sci.*, 1996, **31**, p 707–711